

WZ Production at $e\gamma$ Colliders and Anomalous Quartic $WWZ\gamma$ Coupling

İ. Şahin*

*Department of Physics, Faculty of Sciences,
Ankara University, 06100 Tandogan, Ankara, Turkey*

Abstract

We investigate the constraints on the anomalous quartic $W^+W^-Z\gamma$ gauge boson coupling through the process $e^-\gamma \rightarrow \nu_e W^- Z$. Considering incoming beam polarizations and the longitudinal and transverse polarization states of the final W and Z boson we find 95% confidence level limits on the anomalous coupling parameter a_n with an integrated luminosity of 500 fb^{-1} and $\sqrt{s}=0.5, 1\text{ TeV}$ energies. We show that initial beam and final state polarizations improve the sensitivity to the anomalous coupling by up to factors of 2 - 3.5 depending on the energy.

PACS numbers: 12.15.Ji, 12.60.Cn, 13.88.+e

*isahin@science.ankara.edu.tr

I. INTRODUCTION

The Standard Model (SM) has been a pillar of particle physics. It was subjected to many experimental tests but SM has overcome so many of these experimental and theoretical conflicts. In the recent experiments at CERN e^+e^- collider LEP and Fermilab Tevatron SM of electroweak interactions have been tested with a good accuracy and the experimental results confirms the $SU_L(2) \times U_Y(1)$ gauge structure of the SM. However, Higgs bosons have not been observed and one of the main goals of future experiments is to pursue its trace. SM is largely silent on the issue of the origin of the Higgs boson and many physicists believe that nature might use a more elegant way to accomplish symmetry breaking and mass generation. These kind of considerations motivate us to keep the trace of a more fundamental theory (new physics) in which SM would be embedded.

Self-interactions of gauge bosons have not been tested with a good accuracy and their precision measurements are in the scope of future experiments. Precision measurements of these couplings will be the crucial test of the structure of the SM. Deviation of the couplings from the expected values would indicate the existence of new physics beyond the SM. In this work we analyzed genuinely quartic $W^+W^-Z\gamma$ coupling which do not induce new trilinear vertices. Genuine quartic couplings are contact interactions, manifestations of the exchange of heavy particles. They have different origins than anomalous trilinear couplings. Trilinear couplings are form factors where heavy fields are integrated out at the one-loop level. Therefore it is reasonable to assume that quartic couplings are modified by genuine anomalous interactions while the trilinear couplings are all given by their SM values.

In writing effective operators associated to genuinely quartic couplings we employ the formalism of [1]. Imposing custodial $SU(2)_{Weak}$ symmetry and local $U(1)_{em}$ symmetry, dimension 6 effective lagrangian for the $W^+W^-Z\gamma$ coupling is given by,

$$\mathcal{L}_n = \frac{i\pi\alpha}{4\Lambda^2} a_n \epsilon_{ijk} W_{\mu\alpha}^{(i)} W_{\nu}^{(j)} W^{(k)\alpha} F^{\mu\nu} \quad (1)$$

where $W^{(i)}$ is the $SU(2)_{Weak}$ triplet, and $F_{\mu\nu}$ and $W_{\mu\alpha}^{(i)}$ are the electromagnetic and $SU(2)_{Weak}$ field strengths respectively. a_n is the dimensionless anomalous coupling constant. For sensitivity calculations to the anomalous coupling we set the new physics energy scale Λ to M_W . The vertex function for $W^+(p_+^\mu)W^-(p_-^\nu)Z(p_1^\alpha)\gamma(p_2^\beta)$ generated from the effective lagrangian (1) is given by

$$\begin{aligned}
& i \frac{\pi \alpha}{4 \cos \theta_W \Lambda^2} a_n [g_{\mu\alpha} [g_{\nu\beta} p_{2\cdot} (p_1 - p_+) - p_{2\nu} (p_1 - p_+)_{\beta}] \\
& \quad - g_{\nu\alpha} [g_{\mu\beta} p_{2\cdot} (p_1 - p_-) - p_{2\mu} (p_1 - p_-)_{\beta}] \\
& \quad + g_{\mu\nu} [g_{\alpha\beta} p_{2\cdot} (p_+ - p_-) - p_{2\alpha} (p_+ - p_-)_{\beta}] \\
& \quad - p_{1\mu} (g_{\nu\beta} p_{2\alpha} - g_{\alpha\beta} p_{2\nu}) + p_{1\nu} (g_{\mu\beta} p_{2\alpha} - g_{\alpha\beta} p_{2\mu}) \\
& \quad - p_{-\alpha} (g_{\mu\beta} p_{2\nu} - g_{\nu\beta} p_{2\mu}) + p_{+\alpha} (g_{\nu\beta} p_{2\mu} - g_{\mu\beta} p_{2\nu}) \\
& \quad - p_{+\nu} (g_{\alpha\beta} p_{2\mu} - g_{\mu\beta} p_{2\alpha}) + p_{-\mu} (g_{\alpha\beta} p_{2\nu} - g_{\nu\beta} p_{2\alpha})] \tag{2}
\end{aligned}$$

For a convention, we assume that all the momenta are incoming to the vertex. It should be noted that lagrangian (1) represents only the anomalous $W^+W^-Z\gamma$ coupling. In the cross section calculations one should consider the lagrangian $\mathcal{L} = \mathcal{L}_{SM} + \mathcal{L}_n$ where \mathcal{L}_{SM} is the SM lagrangian for the vertex $W^+W^-Z\gamma$. Therefore within the SM, $a_n = 0$.

CERN e^+e^- collider LEP provide present collider limits on anomalous quartic $W^+W^-Z\gamma$ coupling. At LEP the scaled anomalous coupling $\frac{a_n}{\Lambda^2}$ is constrained by analysing the process $e^+e^- \rightarrow W^+W^-\gamma$. This process is sensitive to anomalous quartic gauge couplings in both $W^+W^-Z\gamma$ and $W^+W^-\gamma\gamma$. Recent results from L3, OPAL and DELPHI collaborations for $W^+W^-Z\gamma$ coupling are given by $-0.14 \text{ GeV}^{-2} < \frac{a_n}{\Lambda^2} < 0.13 \text{ GeV}^{-2}$, $-0.16 \text{ GeV}^{-2} < \frac{a_n}{\Lambda^2} < 0.15 \text{ GeV}^{-2}$ and $-0.18 \text{ GeV}^{-2} < \frac{a_n}{\Lambda^2} < 0.14 \text{ GeV}^{-2}$ at 95% C.L. respectively [2].

There have been several studies in the literature for anomalous quartic $W^+W^-Z\gamma$ coupling through the processes $e^+e^- \rightarrow W^+W^-Z, W^+W^-\gamma, W^+W^-(\gamma) \rightarrow 4f\gamma$ [3], $e\gamma \rightarrow eW^+W^-, \nu_e W^-Z$ [1] and $\gamma\gamma \rightarrow W^+W^-Z$ [4]. In the most of these studies mentioned above future International Linear Collider (ILC) and its $e\gamma$ and $\gamma\gamma$ modes have also been considered. At the $e\gamma$ mode of ILC anomalous $W^+W^-Z\gamma$ coupling appears in eW^+W^- and $\nu_e W^-Z$ production processes. As stated in ref.[1] $\nu_e W^-Z$ production is much more sensitive to anomalous coupling. Another advantage of $\nu_e W^-Z$ production is that it isolates the $W^+W^-Z\gamma$ coupling. This feature is not seen in any other processes mentioned above.

The LHC will start operating soon. A detailed analysis of bosonic quartic couplings at the LHC via the processes $qq \rightarrow qq\gamma\gamma$ and $qq \rightarrow qq\gamma Z (\rightarrow l^+l^-)$ have been done in ref.[5]. The former process receives contributions from the anomalous quartic couplings $ZZ\gamma\gamma$ and $W^+W^-\gamma\gamma$ and the latter receives contributions from $ZZZ\gamma$ and $W^+W^-Z\gamma$ [5]. It was shown that sensitivity bounds to the anomalous quartic $W^+W^-Z\gamma$ coupling through

the process $qq \rightarrow qq\gamma Z(\rightarrow l^+l^-)$ are about the order of $O(10^{-6})$. However, the process $qq \rightarrow qq\gamma Z(\rightarrow l^+l^-)$ does not isolate $W^+W^-Z\gamma$ coupling and the bounds were obtained under the assumption that only one anomalous coupling is different from zero [5].

In this work we consider the process $e\gamma \rightarrow \nu_e W^- Z$ to investigate $W^+W^-Z\gamma$ coupling. This process was analyzed in ref.[1] with unpolarized beams. We take account of incoming beam polarizations and also the longitudinal and transverse polarization states of the final gauge bosons in the cross section calculations to improve the bounds, assuming the polarization of W and Z can be measured [6].

II. CROSS SECTIONS FOR POLARIZED BEAMS

The process $e\gamma \rightarrow \nu_e W^- Z$ takes part as a subprocess in e^+e^- collision. Real gamma beam which enters the subprocess is obtained by Compton backscattering of laser light off linear electron or positron beam where most of the photons are produced at the high energy region.

The spectrum of backscattered photons in connection with helicities of initial laser photon and electron is [7]:

$$f_{\gamma/e}(y) = \frac{1}{g(\zeta)} \left[1 - y + \frac{1}{1-y} - \frac{4y}{\zeta(1-y)} + \frac{4y^2}{\zeta^2(1-y)^2} + \lambda_0 \lambda_e r \zeta (1-2r)(2-y) \right] \quad (3)$$

where

$$g(\zeta) = g_1(\zeta) + \lambda_0 \lambda_e g_2(\zeta) \quad (4)$$

$$g_1(\zeta) = \left(1 - \frac{4}{\zeta} - \frac{8}{\zeta^2} \right) \ln(\zeta + 1) + \frac{1}{2} + \frac{8}{\zeta} - \frac{1}{2(\zeta + 1)^2}$$

$$g_2(\zeta) = \left(1 + \frac{2}{\zeta} \right) \ln(\zeta + 1) - \frac{5}{2} + \frac{1}{\zeta + 1} - \frac{1}{2(\zeta + 1)^2} \quad (5)$$

Here $r = y/[\zeta(1-y)]$ and $\zeta = 4E_e E_0/M_e^2$. E_0 and λ_0 are the energy and helicity of initial laser photon and E_e and λ_e are the energy and the helicity of initial electron beam before Compton backscattering. y is the fraction which represents the ratio between the scattered photon and initial electron energy for the backscattered photons moving along the initial electron direction. Maximum value of y reaches 0.83 when $\zeta = 4.8$ in which the

backscattered photon energy is maximized without spoiling the luminosity. Backscattered photons are not in fixed helicity states their helicities are described by a distribution :

$$\xi(E_\gamma, \lambda_0) = \frac{\lambda_0(1-2r)(1-y+1/(1-y)) + \lambda_e r \zeta[1+(1-y)(1-2r)^2]}{1-y+1/(1-y)-4r(1-r)-\lambda_e \lambda_0 r \zeta(2r-1)(2-y)} \quad (6)$$

The helicity dependent differential cross section for the subprocess can be connected to initial laser photon helicity λ_0 and initial electron beam polarization P_e through the formula,

$$\begin{aligned} d\hat{\sigma}(\lambda_0, P_e; \lambda_W, \lambda_Z) &= \frac{1}{4}(1-P_e) [(1+\xi(E_\gamma, \lambda_0))d\hat{\sigma}(+, L; \lambda_W, \lambda_Z) + (1-\xi(E_\gamma, \lambda_0))d\hat{\sigma}(-, L; \lambda_W, \lambda_Z)] \\ &+ \frac{1}{4}(1+P_e) [(1+\xi(E_\gamma, \lambda_0))d\hat{\sigma}(+, R; \lambda_W, \lambda_Z) + (1-\xi(E_\gamma, \lambda_0))d\hat{\sigma}(-, R; \lambda_W, \lambda_Z)] \quad (7) \end{aligned}$$

Here $d\hat{\sigma}(\lambda_\gamma, \sigma; \lambda_W, \lambda_Z)$ is the helicity dependent differential cross section in the helicity eigenstates; $\sigma : L, R$, $\lambda_\gamma = +, -$ and $\lambda_W, \lambda_Z = +, -, 0$. It should be noted that P_e and λ_e refer to different beams. P_e is the electron beam polarization which enters the subprocess but λ_e is the polarization of initial electron beam before Compton backscattering. The integrated cross section can be obtained by integrating the cross section (7) for the subprocess over the backscattered photon spectrum.

The process $e^- \gamma \rightarrow \nu_e W^- Z$ is described by nine tree-level diagrams. Only the t-channel W exchange diagram contains anomalous $W^+ W^- Z \gamma$ coupling. The helicity amplitudes have been calculated using vertex amplitude techniques derived in ref.[8] and the phase space integrations have been performed by GRACE [9] which uses a Monte Carlo routine.

In our calculations we accept that initial electron beam polarizability is $|\lambda_e|, |P_e|=0.8$. To see the influence of initial beam polarization, energy distributions of backscattered photons $f_{\gamma/e}$ are plotted for $\lambda_e \lambda_0=0, -0.8$ and $+0.8$ in Fig. 1. We see from the figure that backscattered photon distribution is very low at high energies in $\lambda_e \lambda_0=+0.8$. Therefore we will only consider the case $\lambda_e \lambda_0 < 0$ in the cross section calculations. Moreover the Feynman diagram containing anomalous $W^+ W^- Z \gamma$ coupling is a W exchange diagram with a $W e \nu_e$ vertex. Due to V-A structure of the $W e \nu_e$ vertex, $d\hat{\sigma}(\lambda_\gamma, L; \lambda_W, \lambda_Z)$ is more sensitive to anomalous coupling than $d\hat{\sigma}(\lambda_\gamma, R; \lambda_W, \lambda_Z)$. So we will consider the case in which $P_e=-0.8$ (see eq. (7)).

One can see from Fig. 2- 3 the influence of the final state polarizations on the deviations of the total cross sections from their SM value for initial beam polarizations $(\lambda_e, \lambda_0, P_e) =$

$(-0.8, 1, -0.8)$ and $(\lambda_e, \lambda_0, P_e) = (0.8, -1, -0.8)$. In these figures TR and LO stand for "transverse" and "longitudinal" respectively. Transverse polarization configuration of the final bosons are almost insensitive to anomalous coupling. Therefore we omit them in the figures. It is clear from Fig. 2- 3 that longitudinally polarized cross sections are sensitive to anomalous coupling. For instance in Fig. 2 cross section at the polarization configuration $(\lambda_W, \lambda_Z)=(\text{LO}, \text{LO})$ increases by a factor of 3.6 as a_n increases from 0 to 1. But this increment is only a factor of 1.2 in the unpolarized case.

In Fig. 4 longitudinally polarized total cross sections are plotted as a function of anomalous coupling a_n for different initial beam polarizations. Center of mass energy of the e^+e^- system is $\sqrt{s} = 0.5$ TeV. We see from the Fig. 4 the effect of initial beam polarizations on the deviations of cross sections from the SM.

III. ANGULAR CORRELATIONS FOR FINAL STATE FERMIONS

Angular distributions of W^- and Z decay products have clear correlations with the helicity states of these final state gauge bosons. Therefore in principle, polarization states of final W^- and Z boson can be determined by measuring the angular distributions of W^- and Z decay products. This kind of treatment was done in reference [10] for final state W^- and W^+ bosons. Let us consider the differential cross section for the complete process,

$$\begin{aligned}
e^-(k_1, \sigma) + \gamma(k_2, \lambda_\gamma) &\rightarrow \nu_e(q_1, \bar{\sigma}) + W^-(q_2, \lambda_W) + Z(q_3, \lambda_Z) \\
W^-(q_2, \lambda_W) &\rightarrow f_1(p_1, \sigma_1)\bar{f}_2(p_2, \sigma_2) \\
Z(q_3, \lambda_Z) &\rightarrow f_3(p_3, \sigma_3)\bar{f}_4(p_4, \sigma_4)
\end{aligned} \tag{8}$$

with massless fermions $f_1, \bar{f}_2, f_3, \bar{f}_4$. Here σ and λ_γ are the incoming electron and photon helicities; $\bar{\sigma}$, λ_W and λ_Z are the outgoing ν_e , W^- and Z helicities. σ_i represent the helicities of final fermions f_i or \bar{f}_i .

The full amplitude can be expressed as follows:

$$\begin{aligned}
M(k_1, \sigma; k_2, \lambda_\gamma; q_1, \bar{\sigma}; p_i, \sigma_i) &= D_W(q_2^2) D_Z(q_3^2) \sum_{\lambda_W} \sum_{\lambda_Z} M_1(k_1, \sigma; k_2, \lambda_\gamma; q_1, \bar{\sigma}; q_2, \lambda_W; q_3, \lambda_Z) \\
&\times M_2(q_2, \lambda_W; p_1, \sigma_1; p_2, \sigma_2) \times M_3(q_3, \lambda_Z; p_3, \sigma_3; p_4, \sigma_4) \tag{9}
\end{aligned}$$

where $M_1(k_1, \sigma; k_2, \lambda_\gamma; q_1, \bar{\sigma}; q_2, \lambda_W; q_3, \lambda_Z)$ is the production amplitude; helicity amplitudes for $e^- \gamma \rightarrow \nu_e W^- Z$ with on-shell W^- and Z boson. $M_2(q_2, \lambda_W; p_1, \sigma_1; p_2, \sigma_2)$ and $M_3(q_3, \lambda_Z; p_3, \sigma_3; p_4, \sigma_4)$ are the decay amplitudes of W^- and Z boson to fermions. $D_W(q_2^2)$ and $D_Z(q_3^2)$ are the Breit-Wigner propagator factors for W^- and Z bosons.

In this paper we consider lepton decay channel of final state bosons. Therefore $f_1, \bar{f}_2, f_3, \bar{f}_4$ are leptons. M_2 and M_3 decay amplitudes are most simply expressed in the rest frames of W^- and Z respectively. In the W^- rest frame, four-momenta of W^- decay products f_1 and \bar{f}_2 can be parametrized as

$$\begin{aligned} p_1^\mu &= \frac{m_W}{2}(1, \sin\theta\cos\phi, \sin\theta\sin\phi, \cos\theta) \\ p_2^\mu &= \frac{m_W}{2}(1, -\sin\theta\cos\phi, -\sin\theta\sin\phi, -\cos\theta) \end{aligned} \quad (10)$$

where θ and ϕ are polar and azimuthal angles in the W^- rest frame with respect to z-axis defined to be the W^- boson direction in the e^+e^- center of mass frame (lab. frame). W^- rest frame is defined by a boost of the e^+e^- center of mass frame along the z-axis. In this rest frame M_2 decay amplitude is given by

$$M_2 = \frac{g_W}{\sqrt{2}} m_W \delta_{\sigma_1, -} \delta_{\sigma_2, +} l_{\lambda_W} \quad (11)$$

with

$$(l_-, l_0, l_+) = \left(\frac{1}{\sqrt{2}}(1 + \cos\theta)e^{-i\phi}, -\sin\theta, \frac{1}{\sqrt{2}}(1 - \cos\theta)e^{i\phi} \right) \quad (12)$$

In the Z rest frame we parametrize four-momenta of f_3 and \bar{f}_4 as

$$\begin{aligned} p_3^\mu &= \frac{m_Z}{2}(1, \sin\bar{\theta}\cos\bar{\phi}, \sin\bar{\theta}\sin\bar{\phi}, \cos\bar{\theta}) \\ p_4^\mu &= \frac{m_Z}{2}(1, -\sin\bar{\theta}\cos\bar{\phi}, -\sin\bar{\theta}\sin\bar{\phi}, -\cos\bar{\theta}) \end{aligned} \quad (13)$$

where $\bar{\theta}$ and $\bar{\phi}$ are polar and azimuthal angles in the Z rest frame with respect to \bar{z} -axis defined to be the Z boson direction in the e^+e^- center of mass frame. In the Z rest frame M_3 decay amplitude is given by

$$M_3 = m_Z [-g_L \delta_{\sigma_3, -} \delta_{\sigma_4, +} \bar{l}_L(\lambda_Z) + g_R \delta_{\sigma_3, +} \delta_{\sigma_4, -} \bar{l}_R(\lambda_Z)] \quad (14)$$

with

$$\begin{aligned} (\bar{l}_L(-), \bar{l}_L(0), \bar{l}_L(+)) &= \left(\frac{1}{\sqrt{2}}(1 + \cos\bar{\theta})e^{-i\bar{\phi}}, -\sin\bar{\theta}, \frac{1}{\sqrt{2}}(1 - \cos\bar{\theta})e^{i\bar{\phi}} \right) \\ (\bar{l}_R(-), \bar{l}_R(0), \bar{l}_R(+)) &= \left(\frac{1}{\sqrt{2}}(1 - \cos\bar{\theta})e^{-i\bar{\phi}}, \sin\bar{\theta}, \frac{1}{\sqrt{2}}(1 + \cos\bar{\theta})e^{i\bar{\phi}} \right) \end{aligned} \quad (15)$$

$$g_L = g_Z \frac{(C_V + C_A)}{2}, \quad g_R = g_Z \frac{(C_V - C_A)}{2} \quad (16)$$

where C_V and C_A are usual vector and axial vector couplings.

Polarization summed squared matrix elements are given by

$$\sum_{\sigma, \lambda_\gamma, \bar{\sigma}, \sigma_i} |M(k_1, \sigma; k_2, \lambda_\gamma; q_1, \bar{\sigma}; p_i, \sigma_i)|^2 = |D_W(q_2^2)|^2 |D_Z(q_3^2)|^2 P_{\lambda'_W \lambda'_Z}^{\lambda_W \lambda_Z} D_{\lambda'_W}^{\lambda_W} \bar{D}_{\lambda'_Z}^{\lambda_Z} \quad (17)$$

In this equation summation over repeated indices $(\lambda_W, \lambda'_W, \lambda_Z, \lambda'_Z) = +, -, 0$ is implied. $P_{\lambda'_W \lambda'_Z}^{\lambda_W \lambda_Z}$ is the production tensor and $D_{\lambda'_W}^{\lambda_W}, \bar{D}_{\lambda'_Z}^{\lambda_Z}$ are the decay tensors for W and Z boson respectively. They are defined by

$$\begin{aligned} P_{\lambda'_W \lambda'_Z}^{\lambda_W \lambda_Z} &= \sum_{\sigma, \lambda_\gamma, \bar{\sigma}} M_1(k_1, \sigma; k_2, \lambda_\gamma; q_1, \bar{\sigma}; q_2, \lambda_W; q_3, \lambda_Z) \\ &\quad \times M_1^*(k_1, \sigma; k_2, \lambda_\gamma; q_1, \bar{\sigma}; q_2, \lambda'_W; q_3, \lambda'_Z) \end{aligned} \quad (18)$$

$$D_{\lambda'_W}^{\lambda_W} = \sum_{\sigma_1, \sigma_2} M_2(q_2, \lambda_W; p_1, \sigma_1; p_2, \sigma_2) M_2^*(q_2, \lambda'_W; p_1, \sigma_1; p_2, \sigma_2) \quad (19)$$

$$\bar{D}_{\lambda'_Z}^{\lambda_Z} = \sum_{\sigma_3, \sigma_4} M_3(q_3, \lambda_Z; p_3, \sigma_3; p_4, \sigma_4) M_3^*(q_3, \lambda'_Z; p_3, \sigma_3; p_4, \sigma_4) \quad (20)$$

Now let us write down the differential cross section :

$$\begin{aligned} d\sigma &= \frac{1}{2s} |M|^2 \frac{d^3 q_1}{(2\pi)^3 2E_{q_1}} \frac{d^3 p_1}{(2\pi)^3 2E_1} \frac{d^3 p_2}{(2\pi)^3 2E_2} \frac{d^3 p_3}{(2\pi)^3 2E_3} \frac{d^3 p_4}{(2\pi)^3 2E_4} \\ &\quad \times (2\pi)^4 \delta^4(k_1 + k_2 - q_1 - p_1 - p_2 - p_3 - p_4) \end{aligned} \quad (21)$$

Using narrow width approximation it is straightforward to express the differential cross section as

$$d\sigma = \frac{1}{2s}(2\pi)^4\delta^4(k_1 + k_2 - q_1 - q_2 - q_3)\frac{\pi^2}{2^6(2\pi)^6\Gamma_W\Gamma_Zm_Wm_Z} \\ \times P_{\lambda'_W\lambda'_Z}^{\lambda_W\lambda_Z}D_{\lambda'_W}^{\lambda_W}\bar{D}_{\lambda'_Z}^{\lambda_Z}\frac{d^3q_1}{(2\pi)^32E_{q_1}}\frac{d^3q_2}{(2\pi)^32E_{q_2}}\frac{d^3q_3}{(2\pi)^32E_{q_3}}dcos\theta d\phi dcos\bar{\theta}d\bar{\phi} \quad (22)$$

After integration over azimuthal angles ϕ and $\bar{\phi}$ interference terms will vanish and only the diagonal terms $\lambda_W = \lambda'_W$ and $\lambda_Z = \lambda'_Z$ will survive. It is now straightforward to write differential cross section in the form:

$$d\sigma = d\sigma_1(\lambda_W, \lambda_Z)d_{\lambda_W}^{\lambda_W}\bar{d}_{\lambda_Z}^{\lambda_Z}\frac{9}{32(C_V^2 + C_A^2)}B(W \rightarrow l\bar{\nu}_l)B(Z \rightarrow l^+l^-)dcos\theta dcos\bar{\theta} \quad (23)$$

Here $d\sigma_1(\lambda_W, \lambda_Z)$ is the helicity dependent production cross section, $B(W \rightarrow l\bar{\nu}_l)$ and $B(Z \rightarrow l^+l^-)$ are the branching ratios of W and Z boson to leptons. The matrices $d_{\lambda_W}^{\lambda_W}$ and $\bar{d}_{\lambda_Z}^{\lambda_Z}$ are related to the diagonal elements of decay tensors (19-20) as

$$d_{\lambda_W}^{\lambda_W} = l_{\lambda_W}l_{\lambda_W}^* \quad (24)$$

$$\bar{d}_{\lambda_Z}^{\lambda_Z} = [(C_V + C_A)^2\bar{l}_L(\lambda_Z)\bar{l}_L^*(\lambda_Z) + (C_V - C_A)^2\bar{l}_R(\lambda_Z)\bar{l}_R^*(\lambda_Z)] \quad (25)$$

It is difficult to identify nine different polarization configurations of the production cross section but it is sensible to claim that longitudinal (LO) and transverse (TR) polarizations can be identified [10]. Thus we define the following cross sections:

$$d\sigma_1(TR, TR) = \sum_{\lambda_W=+,-} \sum_{\lambda_Z=+,-} d\sigma_1(\lambda_W, \lambda_Z) \quad (26)$$

$$d\sigma_1(LO, LO) = d\sigma_1(0, 0) \quad (27)$$

$$d\sigma_1(TR, LO) = \sum_{\lambda_W=+,-} d\sigma_1(\lambda_W, 0) \quad (28)$$

$$d\sigma_1(LO, TR) = \sum_{\lambda_Z=+,-} d\sigma_1(0, \lambda_Z) \quad (29)$$

$$(30)$$

and

$$d\sigma_1(TR, unpol) = d\sigma_1(TR, TR) + d\sigma_1(TR, LO) \quad (31)$$

$$d\sigma_1(LO, unpol) = d\sigma_1(LO, TR) + d\sigma_1(LO, LO) \quad (32)$$

$$d\sigma_1(unpol, TR) = d\sigma_1(TR, TR) + d\sigma_1(LO, TR) \quad (33)$$

$$d\sigma_1(unpol, LO) = d\sigma_1(TR, LO) + d\sigma_1(LO, LO) \quad (34)$$

For fixed W and Z helicities above cross sections can be obtained from a fit to polar angle distributions of the W and Z decay products in the W and Z rest frames . To be precise for $\lambda_W = \pm 1, 0$ polarization states of final W, production cross sections $d\sigma_1(\pm, \lambda_Z)$ and $d\sigma_1(0, \lambda_Z)$ can be obtained from a fit to d_+^+, d_-^- and d_0^0 distributions in the W rest frame (eqn.(23)). Similarly production cross sections $d\sigma_1(\lambda_W, \pm)$ and $d\sigma_1(\lambda_W, 0)$ can be obtained from a fit to \bar{d}_+^+, \bar{d}_-^- and \bar{d}_0^0 distributions in the Z rest frame. In Fig. 5 and Fig. 6 $d_{\lambda_W}^{\lambda_W}$ and $\bar{d}_{\lambda_Z}^{\lambda_Z}$ distributions are plotted for various polarization states of final W and Z boson. As can be seen from these figures longitudinal (LO) and transverse (TR) distributions are well separated from each other.

There have been several experimental studies in the literature for the measurement of W polarization [6]. It is reasonable to assume that Z polarization can be accessible in a similar manner. At lepton colliders systematic uncertainties are expected to be lower than hadronic colliders. For this reason in our calculations we will ignore the uncertainties associated to the determination of the polarizations of final state gauge bosons.

IV. LIMITS ON THE ANOMALOUS COUPLING PARAMETER

A detailed investigation of the anomalous couplings requires a statistical analysis. To this purpose we have obtained 95% C.L. limits on the anomalous coupling parameter a_n using χ^2 analysis at $\sqrt{s} = 0.5, 1$ TeV and integrated luminosity $L_{int} = 500 \text{ fb}^{-1}$ without systematic errors. The number of events are given as $N = AL_{int}\sigma B_W B_Z$ where A is the overall acceptance and B_W and B_Z are the branching ratios of W and Z boson for leptonic channel.

The limits for the anomalous $W^+W^-Z\gamma$ coupling are given on Table I for unpolarized initial beams and unpolarized, transverse and longitudinal polarization states of final W and Z boson with the acceptance $A = 0.85$. One can see from Table I that polarization

configuration $(\lambda_W, \lambda_Z)=(\text{LO}, \text{TR}+\text{LO})$ is most sensitive to anomalous coupling at $\sqrt{s} = 0.5$ TeV. This configuration improves the limits by a factor of 1.3. But at $\sqrt{s} = 1$ TeV polarization configuration $(\lambda_W, \lambda_Z)=(\text{LO}, \text{LO})$ is the most sensitive and improves the limits by a factor of 2.

On Table II and III the initial beam polarizations are also taken into account. One can see from Table II that polarization configurations $(\lambda_0, \lambda_e, \lambda_W, \lambda_Z)=(1, -0.8, \text{LO}, \text{LO})$ or $(1, -0.8, \text{LO}, \text{TR}+\text{LO})$ improves the limits by a factor of 2. Increase in energy highly improves the limits. At $\sqrt{s} = 1$ TeV the most sensitive polarization configuration is $(\lambda_0, \lambda_e, \lambda_W, \lambda_Z)=(1, -0.8, \text{LO}, \text{LO})$ and this configuration improves the limits by a factor of 3.5.

Anomalous $W^+W^-Z\gamma$ coupling was studied in ref.[1] through the same process $e^-\gamma \rightarrow \nu_e W^- Z$ with unpolarized beams. Using statistical significance authors set 3σ bound of $(-1.2, 0.74)$ on the anomalous $W^+W^-Z\gamma$ coupling parameter a_n with an integrated luminosity of 10 fb^{-1} and $\sqrt{s}=0.5$ TeV energy. In order to compare our results with the results of ref.[1] we have calculated 3σ significance bounds with an integrated luminosity of 10 fb^{-1} and $\sqrt{s}=0.5$ TeV energy. For unpolarized beams we have confirmed the result of ref.[1]. The most sensitive results are obtained at the polarization configurations $(\lambda_0, \lambda_e, \lambda_W, \lambda_Z)=(1, -0.8, \text{LO}, \text{LO})$ and $(1, -0.8, \text{LO}, \text{TR}+\text{LO})$. 3σ significance bounds for the polarization configurations $(\lambda_0, \lambda_e, \lambda_W, \lambda_Z)= (1, -0.8, \text{LO}, \text{LO})$ and $(1, -0.8, \text{LO}, \text{TR}+\text{LO})$ are given by $(-0.59, 0.42)$ and $(-0.63, 0.38)$ respectively. Therefore polarization improves the significance bounds of a_n approximately a factor of 1.92 for integrated luminosity $L_{int} = 10 \text{ fb}^{-1}$ and $\sqrt{s}=0.5$ TeV.

The $e\gamma$ mode of ILC with luminosity $L_{int} = 500 \text{ fb}^{-1}$ probes the anomalous $W^+W^-Z\gamma$ coupling with far better sensitivity than the present collider LEP2 experiments. It improves the sensitivity limits by up to a factor of 10^4 with respect to LEP2. This is comparable with the limits which are expected to be obtained at CERN LHC [5]. One prominent advantage of the process $e^-\gamma \rightarrow \nu_e W^- Z$ is that it isolates anomalous $W^+W^-Z\gamma$ coupling. It provides us the opportunity to study $W^+W^-Z\gamma$ coupling independent from $ZZZ\gamma$ as well as $ZZ\gamma\gamma$ and $W^+W^-\gamma\gamma$. In conclusion, experiments with polarized e^+e^- beams and final state polarizations leads to a significant improvement in the sensitivity limits. Although the SM cross sections in the longitudinal polarization configurations of the final W and Z boson are small, sensitivity limits are better than the transverse polarization case.

-
- [1] O. J. P. Eboli, M. C. Gonzalez-Garcia and S. F. Novaes, Nucl. Phys. **B411**, 381 (1994).
- [2] P. Achard *et al.* (L3 Collaboration), Phys. Lett. **B527**, 29 (2002); J. Abdallah *et al.* (DELPHI Collaboration), Eur. Phys. J. **C31**, 139 (2003); G. Abbiendi *et al.* (OPAL Collaboration), Phys. Lett. **B580**, 17 (2004).
- [3] G. Abu Leil and W. J. Stirling, J. Phys. **G21**, 517 (1995); G. Belanger *et al.*, Eur. Phys. J. **C13**, 283 (2000); W. J. Stirling and A. Werthenbach, Eur. Phys. J. **C14**, 103 (2000); A. Denner *et al.*, Eur. Phys. J. **C20**, 201 (2001); G. Montagna *et al.*, Phys. Lett. **B515**, 197 (2001); M. Beyer *et al.*, Eur. Phys. J. **C48**, 353 (2006).
- [4] O. J. P. Eboli, M. B. Magro, P. G. Mercadante and S. F. Novaes, Phys. Rev. **D52**, 15 (1995).
- [5] O. J. P. Eboli, M. C. Gonzalez-Garcia and S. M. Lietti, Phys. Rev. **D69**, 095005 (2004).
- [6] G. Abbiendi *et al.* (OPAL Collaboration), Eur. Phys. J. **C19**, 229 (2001); Phys. Lett. **B585**, 223 (2004); P. Achard *et al.* (L3 Collaboration), Phys. Lett. **B557**, 147 (2003).
- [7] I. F. Ginzburg *et al.*, Nucl. Instrum. Methods **205**, 47 (1983); **219**, 5 (1984); V. I. Telnov, Nucl. Instrum. Methods **A294**, 72 (1990).
- [8] A. Ballestrero and E. Maina, Phys. Lett. **B350**, 225(1995).
- [9] T. Kaneko in *New Computing Techniques in Physics Research*, edited by D. Perret-Gallix, W. Wojcik (Edition du CNRS, Paris, 1990); MINAMI-TATEYA Group, KEK Report No. 92-19, 1993; F. Yuasa *et al.*, Prog. Theor. Phys. Suppl. **138** 18 (2000).
- [10] K. Hagiwara *et al.*, Nucl. Phys. **B282**, 253 (1987).

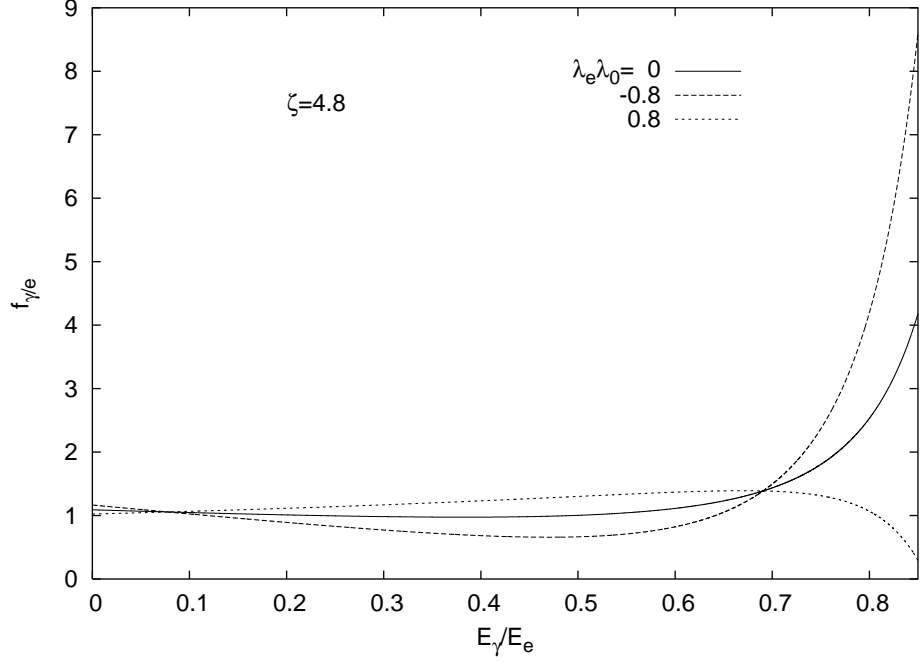


FIG. 1: Energy distribution of backscattered photons for $\lambda_e \lambda_0 = 0, -0.8, 0.8$.

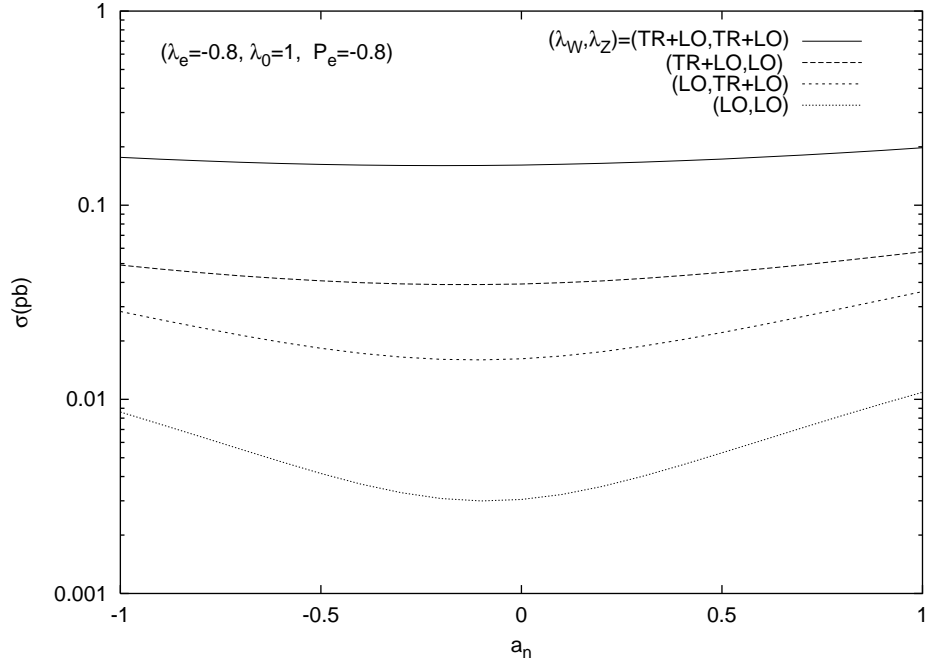


FIG. 2: The integrated total cross section of $e^- \gamma \rightarrow \nu_e W^- Z$ as a function of anomalous coupling a_n for initial beam polarization $(\lambda_e, \lambda_0, P_e) = (-0.8, 1, -0.8)$ and final state polarizations stated on the figure. $\sqrt{s} = 0.5$ TeV.

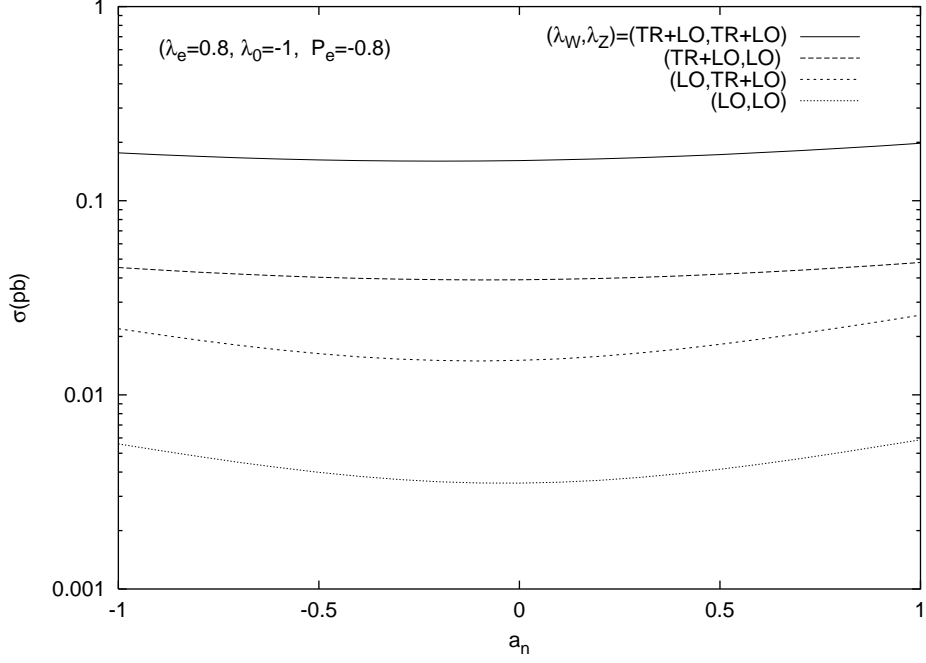


FIG. 3: The same as Fig. 2 but for $(\lambda_e, \lambda_0, P_e) = (0.8, -1, -0.8)$

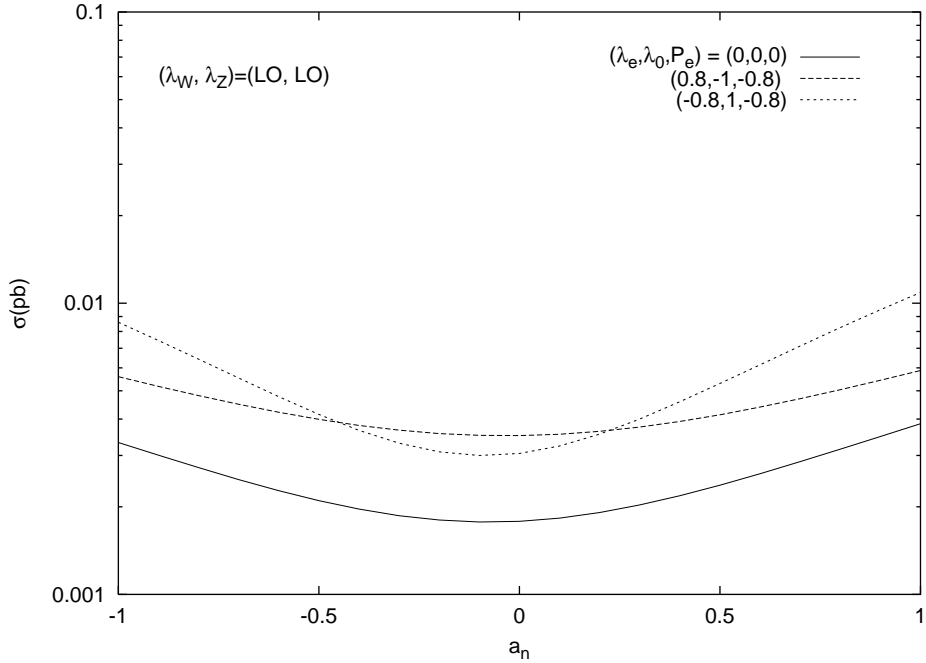


FIG. 4: The integrated total cross section of $e^- \gamma \rightarrow \nu_e W^- Z$ as a function of anomalous coupling a_n for final state polarization configuration $(\lambda_W, \lambda_Z) = (LO, LO)$. The legends are for initial beam polarizations. $\sqrt{s} = 0.5$ TeV.

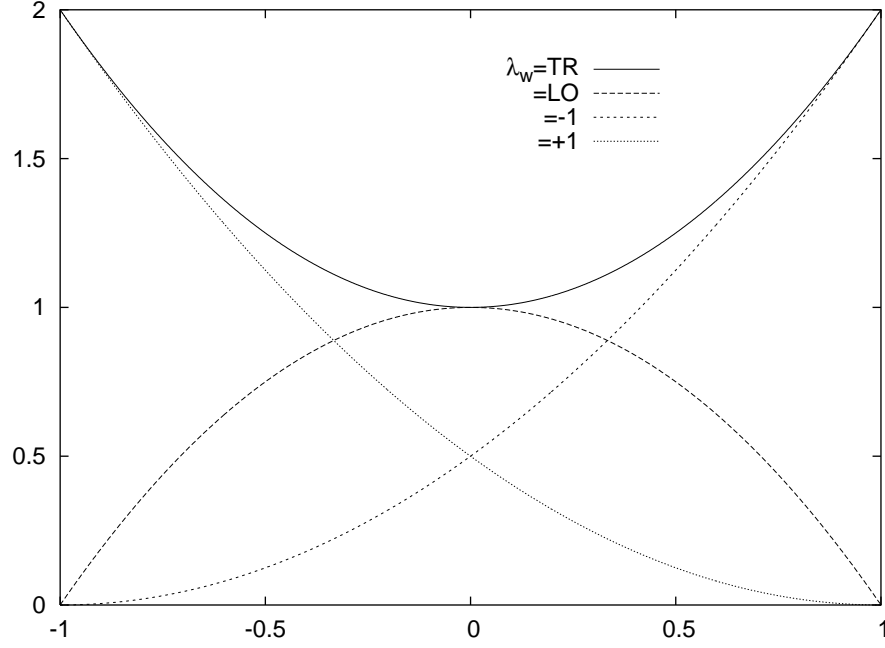


FIG. 5: $d_{\lambda_W}^{\lambda_W}$ versus $\cos\theta$. The legends are for various polarization states of the final W boson.

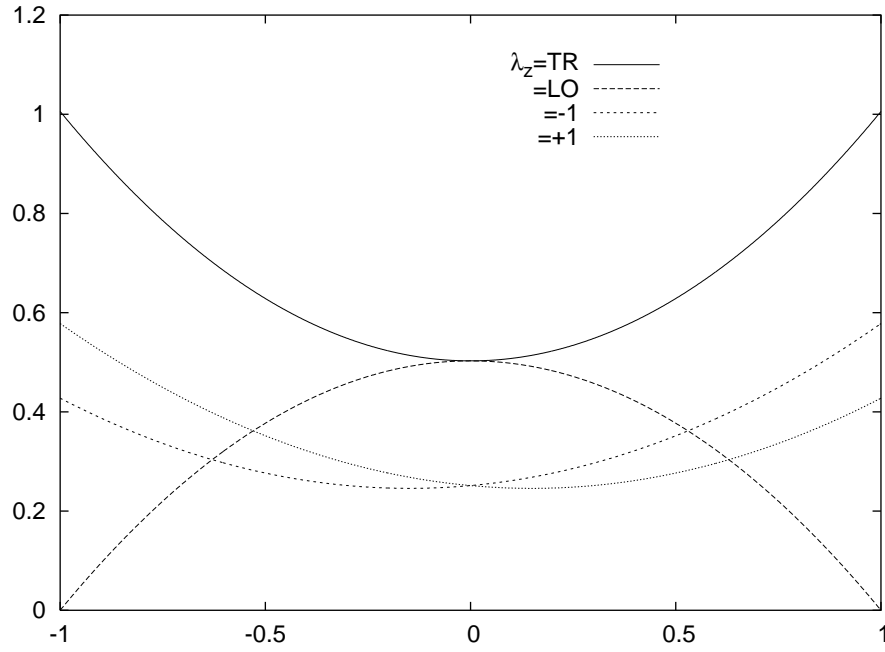


FIG. 6: $\bar{d}_{\lambda_Z}^{\lambda_Z}$ versus $\cos\bar{\theta}$. The legends are for various polarization states of the final Z boson.

TABLE I: Sensitivity of the $e\gamma$ collision to $WWZ\gamma$ couplings at 95% C.L. for $\sqrt{s} = 0.5, 1$ TeV and $L_{int} = 500 \text{ fb}^{-1}$. The initial beams are unpolarized. The effects of final state W and Z boson polarizations are shown in each row.

\sqrt{s} TeV	λ_W	λ_Z	a_n
0.5	TR+LO	TR+LO	-0.95, 0.50
0.5	LO	TR+LO	-0.70, 0.40
0.5	TR	TR+LO	-1.42, 0.75
0.5	TR+LO	LO	-0.87, 0.55
0.5	TR+LO	TR	-1.25, 0.70
0.5	LO	LO	-0.70, 0.55
0.5	TR	TR	-2.60, 1.20
0.5	LO	TR	-0.80, 0.49
0.5	TR	LO	-1.10, 0.70
1	TR+LO	TR+LO	-0.12, 0.09
1	LO	TR+LO	-0.07, 0.06
1	TR	TR+LO	-0.22, 0.17
1	TR+LO	LO	-0.10, 0.09
1	TR+LO	TR	-0.19, 0.14
1	LO	LO	-0.06, 0.05
1	TR	TR	-0.70, 0.40
1	LO	TR	-0.10, 0.08
1	TR	LO	-0.16, 0.13

TABLE II: Sensitivity of the $e\gamma$ collision to $WWZ\gamma$ couplings at 95% C.L. for $\sqrt{s} = 0.5$ TeV and $L_{int} = 500 \text{ fb}^{-1}$. The effects of final state W, Z boson and initial beam polarizations are shown in each row.

λ_0	λ_e	P_e	λ_W	λ_Z	a_n
1	-0.8	-0.8	TR+LO	TR+LO	-0.75, 0.34
1	-0.8	-0.8	LO	TR+LO	-0.50, 0.26
1	-0.8	-0.8	TR	TR+LO	-1.20, 0.52
1	-0.8	-0.8	TR+LO	LO	-0.65, 0.35
1	-0.8	-0.8	TR+LO	TR	-1.02, 0.48
1	-0.8	-0.8	LO	LO	-0.47, 0.29
1	-0.8	-0.8	TR	TR	-2.36, 0.90
1	-0.8	-0.8	LO	TR	-0.61, 0.33
1	-0.8	-0.8	TR	LO	-0.89, 0.47
-1	0.8	-0.8	TR+LO	TR+LO	-0.84, 0.46
-1	0.8	-0.8	LO	TR+LO	-0.60, 0.39
-1	0.8	-0.8	TR	TR+LO	-1.20, 0.65
-1	0.8	-0.8	TR+LO	LO	-0.76 0.57
-1	0.8	-0.8	TR+LO	TR	-1.10, 0.56
-1	0.8	-0.8	LO	LO	-0.70, 0.64
-1	0.8	-0.8	TR	TR	-2.36, 0.98
-1	0.8	-0.8	LO	TR	-0.68, 0.40
-1	0.8	-0.8	TR	LO	-0.90, 0.65

TABLE III: Same as Table II but for $\sqrt{s} = 1$ TeV.

λ_0	λ_e	P_e	λ_W	λ_Z	a_n
1	-0.8	-0.8	TR+LO	TR+LO	-0.08, 0.07
1	-0.8	-0.8	LO	TR+LO	-0.05, 0.04
1	-0.8	-0.8	TR	TR+LO	-0.17, 0.13
1	-0.8	-0.8	TR+LO	LO	-0.07, 0.06
1	-0.8	-0.8	TR+LO	TR	-0.15, 0.11
1	-0.8	-0.8	LO	LO	-0.03, 0.03
1	-0.8	-0.8	TR	TR	-0.62, 0.33
1	-0.8	-0.8	LO	TR	-0.08, 0.06
1	-0.8	-0.8	TR	LO	-0.12, 0.10
-1	0.8	-0.8	TR+LO	TR+LO	-0.11, 0.08
-1	0.8	-0.8	LO	TR+LO	-0.06, 0.05
-1	0.8	-0.8	TR	TR+LO	-0.18, 0.14
-1	0.8	-0.8	TR+LO	LO	-0.10, 0.09
-1	0.8	-0.8	TR+LO	TR	-0.16, 0.11
-1	0.8	-0.8	LO	LO	-0.06, 0.06
-1	0.8	-0.8	TR	TR	-0.63, 0.33
-1	0.8	-0.8	LO	TR	-0.08, 0.06
-1	0.8	-0.8	TR	LO	-0.13, 0.11